arXiv:1612.05216v1 [cond-mat.stat-mech] 15 Dec 2016

Optimal detrended fluctuation analysis as a tool for the determination of the roughness exponent of the mounded surfaces

Edwin E. Mozo Luis,[1,*] Thiago A. de Assis,[1,†] and Silvio C. Ferreira[2,‡]

[1] *Instituto de Física, Universidade Federal da Bahia, Campus Universitário da Federação, Rua Barão de Jeremoabo s/n, 40170-115, Salvador, BA, Brazil*

[2] *Departamento de Física, Universidade Federal de Viçosa, Minas Gerais, 36570-900, Viçosa, Brazil*

(Dated: December 16, 2016)

We present an optimal detrended fluctuation analysis (DFA) and applied it to evaluate the local roughness exponent in non-equilibrium surface growth models with mounded morphology. Our method consists in analyzing the height fluctuations computing the shortest distance of each point of the profile to a detrending curved that fits the surface within the investigated interval. We compare the optimal DFA (ODFA) with both the standard DFA and nondetrended analysis. We validate the ODFA method considering a one-dimensional model in the Kardar-Parisi-Zhang universality class starting from a mounded initial condition. We applied the methods to the Clarke-Vvdensky (CV) model in $2+1$ dimensions with thermally activated surface diffusion and absence of step barriers. It is expected that this model belongs to the nonlinear Molecular Beam Epitaxy (nMBE) universality class. However, an explicit observation of the roughness exponent in agreement with the nMBE class was still missing. The effective roughness exponent obtained with ODFA agrees with the value expected for nMBE whereas using the other methods it does not. We also characterized the transient anomalous scaling of the CV model and found out that the corresponding exponent is in agreement with the value reported for other nMBE models with weaker correction to the scaling.

I. INTRODUCTION

Molecular beam epitaxy (MBE) is a fundamental technique suited to the production of layered materials driven by vapor deposition [1]. In particular, crystal quality requires that each layer is formed before the next one in nonequilibrium surface conditions [1, 2], which is achieved at high adatom mobility. At sufficiently high temperatures, the resulting surfaces can be smooth with global roughness no larger than a few nanometers corresponding to one or two atomic layers.

At moderate temperatures, the interface exhibits kinetic roughening [2, 3]. If the growth is ruled by surface diffusion, it is expected that the dynamics in the hydrodynamic limit is described by the non-linear stochastic equation [3]

$$\frac{\partial h}{\partial t} = -\nu\nabla^4 h + \lambda\nabla^2(\nabla h)^2 + \eta, \tag{1}$$

where $h(\mathbf{r},t)$ is the height at position $\mathbf{r}$ and time t measured perpendicularly to a for d-dimensional substrate, $\eta(\mathbf{r},t)$ is a Gaussian, nonconservative noise given by $\langle\eta\rangle = 0$ and $\langle\eta(\mathbf{r},t)\eta(\mathbf{r}',t')\rangle = D\delta^d(\mathbf{r}-\mathbf{r}')\delta(t-t')$ while ν and λ are constants. This equation was independently proposed by Villain [4] and by Lai and Das Sarma [5] being also known as the Villain-Lai-Das Sarma (VLDS) equation and it is a standard model of the nonlinear molecular beam epitaxy (nMBE) universality class. This equation has been investigated in the framework of renormalization group [6–10] and many features observed in kinetic Monte Carlo simulations have been elucidated.

MBE is often modeled by microscopic transition rules built to capture the atomistic mechanisms. The basic approach is to use stochastic transition rates for atomistic processes such as deposition and thermally activated adatom hopping [11, 12]. A fundamental example in this class is the Clarke-Vvedensky (CV) model [13], in which deposition occurs at a constant and uniform rate and the adatom diffusion rate is given by an Arrhenius law in the form $D = \nu_0 \exp(-E/k_bT)$ where ν_0 is an attempt frequency and E is an energy barrier for the hopping of an adatom with n nearest neighbors (bonds). The activation barrier includes the contribution of the substrate (E_S) as well as of the bonds in the same layer (E_N) assuming the form $E = E_S + nE_N$. Renormalization studies [8–10] point out that the CV model belongs to the nMBE class. The presence of step barriers [1] in the CV model, in which the diffusion between different atomic layers is depleted, asymptotically leads to mounded morphologies with non self-affine structure [12, 14].

Some investigations of the dynamic scaling of the surface roughness in CV-type models have been reported [15–19]. The interface fluctuation within a window of length l (hereafter called quadratic local roughness) is defined as

$$\omega_i^2(l,t) = \langle h^2\rangle_i - \langle h\rangle_i^2, \tag{2}$$

where $\langle\cdots\rangle_i$ means averages over the window i. The quadratic local interface width $\omega^2(l,t)$ is defined as the average of ω_i^2 over different windows and samples. In self-affine dynamical scaling, the local roughness increases as $\omega \sim t^\beta$ for $t \ll l^z$ and saturates as $\omega \sim l^\alpha$ for $t \gg l^z$, with $z = \alpha/\beta$, and these scaling exponents are called growth

* eluis@ufba.br
† thiagoaa@ufba.br
‡ silviojr@ufv.br

(β), roughness (α) and dynamic (z) exponents [3], respectively. If l is chosen to be the system size L, Eq. (2) yields the squared global roughness. Former works on the CV model suggest temperature dependent exponents and anomalous scaling of surface roughness [15–17]. Recently, the local roughness of the CV model in $d = 2$ has been analyzed and transient anomalous (non self-affine) scaling has been found [19]. As a consequence, nMBE asymptotical exponents with large corrections to the scaling were conjectured, for the CV model, in consonance with other nMBE models [20]. Numerical simulations in $d = 2$ of atomistic models in the nMBE class with weaker corrections to the scaling, provide growth and dynamical exponents $\beta \approx 0.2$ and $z \approx 3.33$, respectively [21] in agreement with the one-loop renormalization group exponents $\beta = 1/5$ and $z = 10/3$ for the VLDS equation [4, 5]. These exponents were also found from the scaling analysis of the CV model in Ref. [19].

However, the scaling of the local roughness at small length scales does not provide estimates of the roughness exponent for several irreversible growth models in agreement with the universality classes they belong in both one- and two-dimensional substrates [22]. This caveat was also observed for the CV model in both irreversible [23] and reversible [19] aggregation versions. Then, a direct measurement of the roughness exponent corresponding to CV model is still lacking.

In the present work, we propose a modification of the standard detrended fluctuation analysis (DFA) [24], in which the height fluctuations are reckoned in terms of the shortest distance to a detrending curve, as a method to calculate the roughness exponent of mounded surfaces. The method was validated with a model in the Kardar-Parisi-Zhang (KPZ) [25] universality class growing from mounded initial conditions and applied to the CV model in the regime exhibiting mounded morphologies. Our method was able to capture fluctuations within length scales smaller than the mound sizes, arising as a promising strategy to unveil the universality class of models where the leading contributions to fluctuations are within the mounds. This method also provides evidences of transient anomalous scaling in the CV model with the same characteristic exponent observed for other nMBE models with weaker corrections to the scaling.

The sequence of the paper is organized as follows. In Sec. II, we present basic concepts and definitions of kinetic roughening theory and introduce the optimal DFA (ODFA) method. In Sec. III, we validate the method using the etching model [26], that belongs to the KPZ universality class, for a mounded initial condition. In Section IV, we discuss the formation of rough mounds in CV model and the outcomes obtained with ODFA method comparing them with the DFA and nondetrended methods. Section V summarizes our conclusions.

II. METHODS

A. Dynamical scaling

We will consider the surface evolution in the growth regime where the global roughness scale as $W = \omega(L,t) \sim t^{\beta}$. A characteristic surface length can be extracted from the autocorrelation function defined as

$$\Gamma(\mathbf{r},t) = \langle \tilde{h}(\mathbf{r_0}+\mathbf{r},t)\tilde{h}(\mathbf{r},t)\rangle, \tag{3}$$

where $\tilde{h} = h - \bar{h}$, $\bar{h}$ is the mean height of profile, and averages in Eq. (3) are performed over different reference positions $\mathbf{r_0}$, different orientations and independent samples. Surface growth under nonequilibrium conditions may present mounded morphologies [2, 12, 27]. In mounded surfaces, the characteristic lateral surface length can be estimated as the first zero (ξ_0) or the first minimum (ξ_m) of autocorrelation function [1, 12, 14]. Those lengths are expected to scale as

$$\xi_{0,m} \sim t^{1/z_c}, \tag{4}$$

where z_c is the coarsening exponent that, in case of self-affine growth, corresponds to the dynamical exponent defined previously.

Under the hypothesis of normal (non anomalous [19, 28, 29]) scaling, the local roughness obeys the Family-Vicsek ansatz [30] given by

$$\omega(l,t) \sim t^{\beta} F\left(\frac{l}{t^{1/z}}\right), \tag{5}$$

where F scales as $F(x) \sim x^{\alpha}$ for $x \ll 1$ and $F(x) = \text{const}$ for $x \gg 1$, leading to $\omega \sim t^{\beta}$ for $t \ll l^z$ and $\omega \sim l^{\alpha}$ for $t \gg l^z$. In case of anomalous scaling [31] the local roughness follows the modified ansatz

$$\omega(l,t) \sim t^{\beta} F_{\text{ano}}\left(\frac{l}{t^{1/z}}\right), \tag{6}$$

where $F_{\text{ano}}(x) \sim x^{\alpha_{\text{loc}}}$ if $x \ll 1$ and $F_{\text{ano}}(x) = \text{const}$ for $x \gg 1$. Notice that if $\alpha \neq \alpha_{\text{loc}}$, one has $\omega(l,t) \sim l^{\alpha_{\text{loc}}} t^{\kappa}$, where $\kappa = (\alpha - \alpha_{\text{loc}})/z$ for short scales. Therefore, for anomalous scaling, the amplitude of ω vs l scales as t^{κ}, where κ is the anomaly exponent[19, 28, 29].

B. Optimal DFA

Lets consider the standard DFA method using a nth order polynomial to detrend the surface [24], called here of DFA$_n$. For sake of simplicity, we consider one-dimensional cross sections in case of two-dimensional surfaces. The interface fluctuation within a window i of size l in DFA$_n$ is defined as

$$\omega_i^{(n)} = \langle (\delta^{(n)})^2 \rangle_i^{1/2} \tag{7}$$

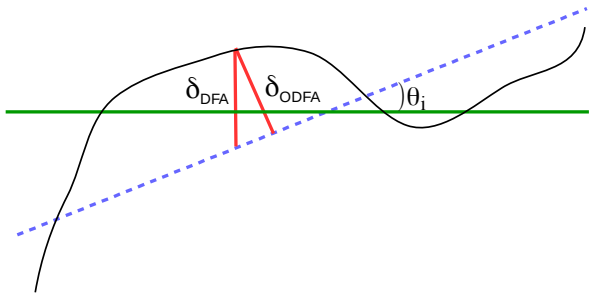

FIG. 1. Schematic representation of DFA_1 and $ODFA_1$ methods. The dashed line represents the linear regression used to detrend the interface and the solid one is parallel to the substrate.

where

$$\delta^{(n)} = h(x) - G_i(x; A_i^{(0)}, A_i^{(1)}, \ldots, A_i^{(n)}) \qquad (8)$$

with G_i being a nth order polynomial regression of the interface in ith window with coefficients $A_i^{(0)}, A_i^{(1)}, \ldots, A_i^{(n)}$ obtained using least-squares method [32]. The local roughness yielded by the DFA_n method $\omega^{(n)}$ is defined considering the average over different windows and samples. We stress that $h(x)$ is the height of the profile with respect to $h = 0$. In the standard local roughness analysis, that corresponds to DFA_0, the surfaces fluctuations are computed in relation to the average height such that $G_i = A_i^{(0)} = \langle h \rangle_i$.

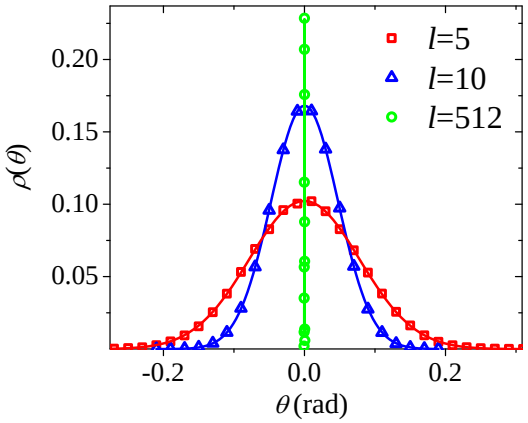

FIG. 2. (Color online) Distributions of the local slope for different window sizes in a surface obtained with the CV model, performed with $L = 1024$, $t = 100$, using parameters $R = 10$ and $\epsilon = 10^{-2}$.

Now, we introduce the ODFA method. The local roughness in the window i of size l is defined as Eq. (7) with

$$\delta^{(n)} = \min\left[h(x) - G_i(x; A_i^{(0)}, A_i^{(1)}, \ldots, A_i^{(n)})\right], \qquad (9)$$

where "min" represents minimal distance from the surface point with height $h(x)$ to the polynomial G_i. Notice that $ODFA_0$ correspond exactly to DFA_0 but for higher orders they are different. In particular, we can easily verify that $\delta^{(1)} = [h(x) - G_i]\cos(\theta_i)$ is the distance to the detrending curve. Figure 1 shows a schematic representation for DFA_1 and $ODFA_1$,. The variable θ_i corresponds to the angle between substrate and the local trend $[\theta_i = \text{atan}(A_i^{(1)})]$. Observe that for $l \gg 1$, both DFA and ODFA correspond to the global roughness given by Eq. (2) with $l = L$, since the whole surface is not trended. Figure 2 shows the probability that a window of size l has slope θ using DFA_1 in a simulation of the CV model (see Sec. IV for simulation details). The distributions are Gaussian and converge to Dirac delta function centered at $\theta = 0$ as l increases. In higher order ODFA, the minimal distance can be computed numerically using root finding algorithms as the bisection method [32], used in the present work.

III. VALIDATING THE ODFA METHOD

In order to validate the ODFA method and compare it with DFA, we consider the deposition on an initially mounded one-dimensional surface shown in Fig. 3(a). The surface evolves according to the etching model rules [26] in $d = 1$, that belongs to the KPZ universality class [25]. This model has a large roughness and also strong corrections to the scaling [33, 34], characteristics that makes it suitable to perform the tests. The model rules are as follows: at each time step, a site $\mathbf{x}$ is randomly chosen and all nearest-neighbors of $\mathbf{x}$ that obey $h(\mathbf{y}) < h(\mathbf{x})$ are increased as $h(\mathbf{y}) \to h(\mathbf{x})$ and subsequently $h(\mathbf{x}) \to h(\mathbf{x}) + 1$. Note that the surface preserves its initially mounded structure ($\xi_0 \simeq 1000$) in the whole interval of simulation considered, as shown by the correlation function in the inset of Fig. 3(a).

Figure 3(b) compares the effective exponent analyses for local interface width using non detrended analysis (DFA_0), DFA and ODFA up to second order. The effective roughness exponent α_{eff} is defined as $\alpha_{\text{eff}} \equiv d\ln(\omega^{(n)})/d\ln(l)$. Using DFA_0 leads to a large exponent typical of mounded surfaces because it is ruled by the long wavelength scales and does not capture the local fluctuations. The DFA_1 analysis provides a plateau on $\alpha_{\text{eff}} = 0.44$ below the exactly known value $\alpha_{\text{KPZ}} = 1/2$ [25]. Using DFA_2, we observe an increasing of the range of plateau but no significant improvement of the exponent value is found. For ODFA method however, we observe a plateau very close to the KPZ exponent 1/2 with a larger plateau for $ODFA_2$. We stress that, in the larger scale length limit (larger than the average mound length), the values of the effective roughness exponent reflect the geometrical aspects of the mounded surface, i.e. $\alpha_{\text{eff}} > 0.5$ is expected.

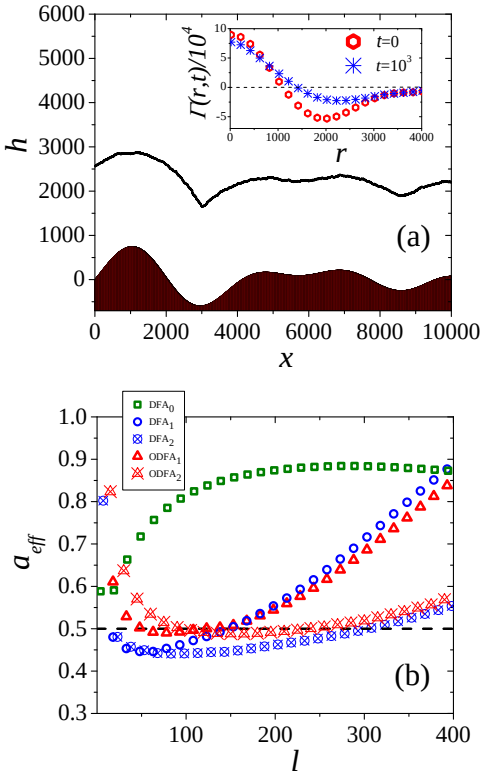

FIG. 3. (Color online) (a) Mounded initial condition and the (shifted) profile after a deposition time $t = 10^3$ using Etching model. The corresponding correlation functions are shown in the inset. (b) Effective local roughness exponent as a function of the window size for a deposition time $t = 10^3$ using different methods. The horizontal dashed line indicates the value of the KPZ roughness exponent $\alpha_{\rm KPZ} = 1/2$.

IV. RESULTS FOR CV MODEL IN D=2

We performed simulations of the CV model in a simple cubic lattice, with an initially flat substrate at $h = 0$ with lateral size L. Periodic boundaries conditions along the substrate directions are considered. Deposition occurs with a flux normal to the substrate of F atoms per site per unit of time under a solid-on-solid condition. The ratio

$$R \equiv \frac{D_0}{F}, \tag{10}$$

in which $D = D_0\epsilon^n$ is the hopping rate if an adatom has n lateral neighbors, is a control parameter of the model. Here, $D_0 = \nu_0 \exp(-E_s/k_BT)$ is the hopping rate of an adatom with no lateral bond, and $\epsilon = \exp(-E_N/k_BT)$. One time unit corresponds to the deposition of L^2 adatoms, fixing $F = 1$ without loss of generality. In a deposition event, the atom is adsorbed on the top of the previously deposited adatom or the substrate site to grant the solid-on-solid condition. For the same reason, only adatoms at the top of the columns are mobile and perform random hopping towards the top of their nearest neighbor sites.

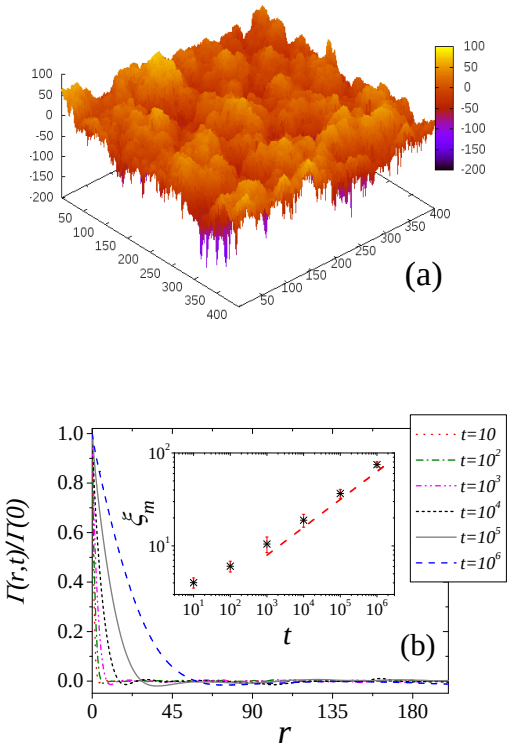

FIG. 4. (Color online) (a) Typical morphology of a surface generated with the CV model, at deposition time $t = 10^6$, showing the formation of mounds. (b) Scaled autocorrelation function $\Gamma(r,t)/\Gamma(0)$ as a function of the distance r. The inset shows the time evolution of the characteristic length given by the minimum of the autocorrelation function. The dashed line has a slope 0.30.

We performed simulations of the CV model for $R = 10$ and $\epsilon = 10^{-2}$, that corresponds to a low temperature regime. This leads to a high surface roughness and allows for a more accurate scaling analysis since the higher temperature regimes are dominated by a layer-by-layer growth [1, 14] during an exceedingly long transient. The substrate has lateral size $L = 1024$, grating that the system is still in the growth regime for the analyzed times. This parameter set was used in all results presented in this work but we stress that other values with the same order of magnitude were studied and the conclusions presented hereafter still holds.

Figure 4(a) shows a typical surface morphology generated by simulations of the CV model after the deposition of 10^6 layers. The average size of the mounds was estimated using the first minimum of the autocorrelation function, as shown in Fig. 4(b). After an initial transient ($t \gtrsim 10^3$), a scaling regime $\xi_m \sim t^{1/z_c}$ is observed with an exponent in agreement with $1/z = 0.3$ of the nMBE class as can be seen in the inset of Fig. 4(b), confirming that this lateral characteristic length has the same scaling as

the correlation length in this regime.

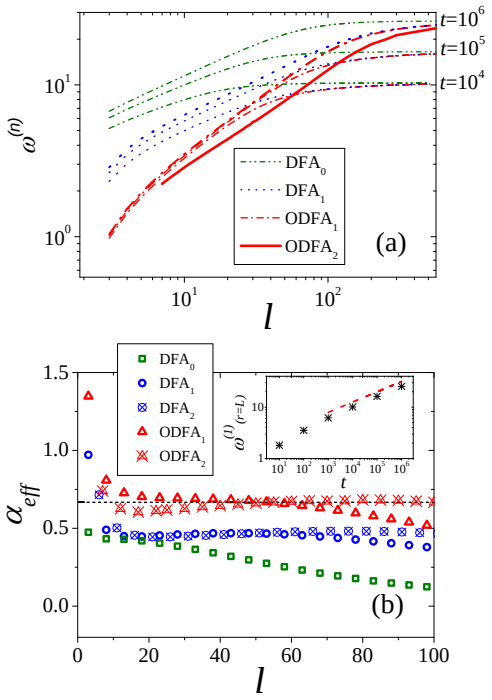

FIG. 5. (Color online) (a) Local roughness using different methods as a function of the window size for different times. (b) Effective local roughness exponent [$\alpha_{\rm eff} \equiv d\ln(\omega^{(n)})/d\ln(l)$] analysis for different methods for a deposition time $t = 10^6$. The horizontal dashed line indicates the value of the nMBE roughness exponent $\alpha_{\rm nMBE} = 2/3$. The inset shows the time evolution of the global roughness obtained with ODFA$_1$ and the dashed line has slope 0.20.

Figure 5(a) compares the local roughnesses using DFA with ODFA methods at different times. In Fig. 5(b), the effective roughness exponent is shown as a function of l for $t = 10^6$. The analysis for ODFA$_1$ provides a plateau for $\alpha_{\rm eff} \approx 2/3$ for the size range $25 \lesssim l \lesssim 60$ with a larger plateau for ODFA$_2$. We can see, for the time intervals considered, that DFA up second order provide estimates of roughness exponent bellow the value expected for nMBE class. Only the sizes of the plateaus are increased for DFA$_2$ similarly to the behavior observed for the etching model in Fig. 3.

From Fig. 4(b), we obtain that the average size of the mounds at $t = 10^6$ is $\xi_m \approx 75$. Therefore, ODFA methods indicate that nMBE roughness exponent can be extracted from the CV model considering fluctuations with optimal (minimal) distance to the local trending, in scales up to the same order of the size of the mounds. This result is particularly useful and raises the possibility of measuring the roughness exponent for experimentally accessible times. The inset of Fig 5(b) shows the global roughness against time computed using ODFA$_1$ (similarly for DFA and ODFA$_2$) for $l = L$. The results provide $\omega \sim t^{0.2}$ for $t \gtrsim 10^3$, which is fully consistent with the nMBE growth exponent and confirm the predictions.

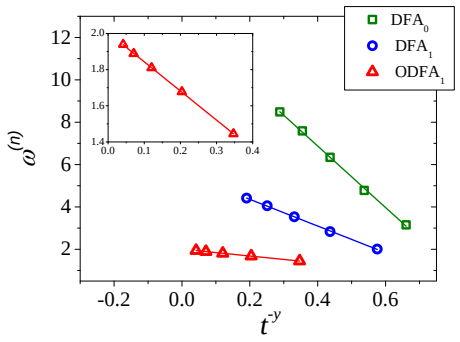

FIG. 6. (Color online) Transient anomalous scaling analysis for the CV model using different methods: DFA$_0$, DFA$_1$ and ODFA$_1$ with $y = 0.09$, 0.12, and 0.23, respectively. The window size used to compute the local roughness is $l = 5$. The inset represents a zoom of the vertical scale improving the visibility of the ODFA$_1$ curve.

Now, we address the transient anomalous scaling of the CV model. In self-affine (non anomalous) scaling, the local roughness, at very short scales (of order of just a few lattice spaces) approaches a finite value at long times following a power-law corrections as

$$\omega^{(0)} = C_1 + C_2 t^{-y}, \tag{11}$$

where C_1 and C_2 are constants. This is the the same behavior of the squared average local slope $|(\nabla h)|^2$ [20]. For the Edwards-Wilkinson (EW) [35] and KPZ [25] equations, the values of the exponent y were computed analytically as $y_{\rm EW} = d/2$ and $y_{\rm KPZ} = 2(1-\alpha)/z$, respectively [36, 37]. In Ref.[19], it was shown that the effective anomaly exponent in the range $0.08 \leq \kappa \leq 0.23$ observed for the CV model, is due to a transient effect since the local roughness for a very small scale approaches a constant value according Eq. (11) with $y = 0.09$.

The local roughness for a window of size $l = 5$ is shown as a function of t^{-y} in Fig. 6 for DFA$_0$, DFA$_1$ and ODFA$_1$, considering $y = 0.09$, 0.12 and 0.23, respectively, showing that the convergence to a constant value is quicker for ODFA$_1$. This is an additional evidence that CV model exhibits asymptotically normal scaling, corroborating conjecture of Ref. [20] where other models of the nMBE class were investigated. It is worth noticing that the exponent $y = 0.23$ found with ODFA$_1$ is the same found in the conserved restricted solid-on-solid (CRSOS) model [20], where scaling corrections are weaker.

Finally, we notice that ODFA$_n$, with $n \geq 1$, also works for self-affine surfaces, and improved results were obtained as compared with DFA$_0$. However, no significant differences were observed as compared with DFA$_n$. Therefore, we propose that using ODFA in experimental

procedures is strongly indicated since it is equivalent to standard DFA in self-affine growth but captures better the nature of the fluctuations in case of mounded surfaces.

V. CONCLUSIONS

In this work we have investigated a detrended fluctuation analysis, in which the height fluctuations are taken with respect to the optimal (minimal) distance from the detrending curve. This modification was observed to be irrelevant for the determination of the roughness exponents of purely self-affine surfaces but we observed that it becomes relevant for systems with transient mounded behavior, which encompasses models belonging to the important universality class of non-linear molecular beam epitaxy. The method was validated and compared with standard DFA analysis using an one-dimensional growth model with a well-known roughness exponent.

We applied the method to the Clarke-Vvdensky model where deposition competes with thermally activated surface diffusion producing interfaces with rough mounds. Since this model possesses the central mechanisms of the nMBE class, it is expected to exhibit the nMBE exponents. We compared the present method with non detrended and standard DFA analyses for the CV model at low temperature and long times. A roughness exponent in agreement with the nMBE universality class ($\alpha_{\text{nMBE}} = 2/3$) was observed only for ODFA. We also investigated the transient anomalous scaling, in which the local roughness within small windows converges to a constant value with a power law correction in time, Eq. (11), and found that the ODFA method yields the same exponent $y = 0.23$ observed for other nMBE models with weaker correction to the scaling [20]. Since this exponent is universal for other universality classes, namely EW and KPZ [36, 37], our results point that the same holds for the nMBE class.

We expect that our results will be of relevance for experimental analyses, in which mounded morphologies are commonly observed [1] and the resolution of the universality class is challenging. As perspectives, would be interesting to consider the role of the intrinsic smoothening of the surface in case of profiles obtained by the widely used scanning probe microscopy techniques that can markedly interfere in the roughness exponent determination [38] or even indicate a misleading universality class [39].

ACKNOWLEDGEMENTS

The authors acknowledge the financial support of the Conselho Nacional de Desenvolvimento Científico e Tecnológico (CNPq). SCF thanks the financial support of Fundação de Amparo à Pesquisa do Estado de Minas Gerais (FAPEMIG). EEML acknowledges the support by Coordenação de Aperfeiçoamento de Pessoal de Nível Superior (CAPES). TAdA acknowledges F. D. A. Aarão Reis for fruitful discussions.

[1] J. Evans, P. Thiel, and M. Bartelt, "Morphological evolution during epitaxial thin film growth: Formation of 2D islands and 3D mounds," Surf. Sci. Rep. **61**, 1 (2006).

[2] T. Michely and J. Krug, *Islands, Mounds and Atoms*, Springer Series in Surface Sciences (Springer Berlin Heidelberg, 2012).

[3] A. Barabási and H. Stanley, *Fractal Concepts in Surface Growth* (Cambridge University Press, 1995).

[4] J. Villain, "Continuum models of crystal growth from atomic beams with and without desorption," J. Phys. I **1**, 19 (1991).

[5] Z.-W. Lai and S. Das Sarma, "Kinetic growth with surface relaxation: Continuum versus atomistic models," Phys. Rev. Lett. **66**, 2348 (1991).

[6] H. K. Janssen, "On critical exponents and the renormalization of the coupling constant in growth models with surface diffusion," Phys. Rev. Lett. **78**, 1082 (1997).

[7] T. Singha and M. K. Nandy, "A renormalization scheme and skewness of height fluctuations in (1 + 1)-dimensional VLDS dynamics," J. Stat. Mech. , 023205 (2016).

[8] C. A. Haselwandter and D. D. Vvedensky, "Fluctuation regimes of driven epitaxial surfaces," Europhys. Lett. **77**, 38004 (2007).

[9] C. A. Haselwandter and D. D. Vvedensky, "Renormalization of stochastic lattice models: Epitaxial surfaces," Phys. Rev. E **77**, 061129 (2008).

[10] C. A. Haselwandter and D. D. Vvedensky, "Renormalization of Atomistic Growth Models," Int. J. Modern Phys. B **22**, 3721 (2008).

[11] D. D. Vvedensky, "Multiscale modelling of nanostructures," J. Phys.: Cond. Matt. **16**, R1537 (2004).

[12] F. F. Leal, S. C. Ferreira, and S. O. Ferreira, "Modelling of epitaxial film growth with an Ehrlich-Schwoebel barrier dependent on the step height," J. Phys.: Cond. Matt. **23**, 292201 (2011).

[13] S. Clarke and D. D. Vvedensky, "Growth kinetics and step density in reflection high-energy electron diffraction during molecular-beam epitaxy," J. Appl. Phys. **63**, 2272 (1988).

[14] F. F. Leal, T. J. Oliveira, and S. C. Ferreira, "Kinetic modelling of epitaxial film growth with up- and downward step barriers," J. Stat. Mech. , P09018 (2011).

[15] P. I. Tamborenea and S. Das Sarma, "Surface-diffusion-driven kinetic growth on one-dimensional substrates," Phys. Rev. E **48**, 2575 (1993).

[16] S. Das Sarma, C. J. Lanczycki, R. Kotlyar, and S. V. Ghaisas, "Scale invariance and dynamical correlations in growth models of molecular beam epitaxy," Phys. Rev.

E **53**, 359 (1996).
[17] M. Kotrla and P. Šmilauer, "Nonuniversality in models of epitaxial growth," Phys. Rev. B **53**, 13777 (1996).
[18] B. Meng and W. Weinberg, "Dynamical monte carlo studies of molecular beam epitaxial growth models: interfacial scaling and morphology," Surf. Sci. **364**, 151 (1996).
[19] T. A. de Assis and F. D. A. Aarão Reis, "Dynamic scaling and temperature effects in thin film roughening," J. Stat. Mech , P06023 (2015).
[20] F. D. A. Aarão Reis, "Normal dynamic scaling in the class of the nonlinear molecular-beam-epitaxy equation," Phys. Rev. E **88**, 022128 (2013).
[21] F. D. A. Aarão Reis, "Numerical study of discrete models in the class of the nonlinear molecular beam epitaxy equation," Phys. Rev. E **70**, 031607 (2004).
[22] A. Chame and F. Aarão Reis, "Scaling of local interface width of statistical growth models," Surf. Sci. **553**, 145 (2004).
[23] T. A. de Assis and F. D. A. Aarão Reis, "Thin film deposition with time-varying temperature," J. Stat. Mech. , P10008 (2013).
[24] C.-K. Peng, S. V. Buldyrev, S. Havlin, M. Simons, H. E. Stanley, and A. L. Goldberger, "Mosaic organization of dna nucleotides," Phys. Rev. E **49**, 1685 (1994).
[25] M. Kardar, G. Parisi, and Y.-C. Zhang, "Dynamic scaling of growing interfaces," Phys. Rev. Lett. **56**, 889 (1986).
[26] B. A. Mello, A. S. Chaves, and F. A. Oliveira, "Discrete atomistic model to simulate etching of a crystalline solid," Phys. Rev. E **63**, 041113 (2001).
[27] K. J. Caspersen, A. R. Layson, C. R. Stoldt, V. Fournee, P. A. Thiel, and J. W. Evans, "Development and ordering of mounds during metal(100) homoepitaxy," Phys. Rev. B **65**, 193407 (2002).
[28] J. M. López, "Scaling approach to calculate critical exponents in anomalous surface roughening," Phys. Rev. Lett. **83**, 4594 (1999).
[29] F. S. Nascimento, S. C. Ferreira, and S. O. Ferreira, "Faceted anomalous scaling in the epitaxial growth of semiconductor films," Europhys. Lett. **94**, 68002 (2011).
[30] F. Family and T. Vicsek, "Scaling of the active zone in the eden process on percolation networks and the ballistic deposition model," J. Phys. A: Math. Gen. **18**, L75 (1985).
[31] J. M. López, M. A. Rodríguez, and R. Cuerno, "Superroughening versus intrinsic anomalous scaling of surfaces," Phys. Rev. E **56**, 3993 (1997).
[32] W. H. Press, S. A. Teukolsky, W. T. Vetterling, and B. P. Flannery, *Numerical Recipes 3rd Edition: The Art of Scientific Computing*, 3rd ed. (Cambridge University Press, New York, NY, USA, 2007).
[33] T. J. Oliveira, S. G. Alves, and S. C. Ferreira, "Kardar-Parisi-Zhang universality class in 2+1 dimensions: Universal geometry-dependent distributions and finite-time corrections," Phys. Rev. E **87**, 040102 (2013), 1302.3750.
[34] I. S. S. Carrasco, K. a. Takeuchi, S. C. Ferreira, and T. J. Oliveira, "Interface fluctuations for deposition on enlarging flat substrates," New J. Phys. **16**, 123057 (2014).
[35] S. F. Edwards and D. R. Wilkinson, "The surface statistics of a granular aggregate," Proc. R. Soc. Lond. A **381**, 17 (1982).
[36] J. Krug and P. Meakin, "Universal finite-size effects in the rate of growth processes," J. Phys. A: Math. Gen. **23**, L987 (1990).
[37] Y.-L. Chou and M. Pleimling, "Kinetic roughening, global quantities, and fluctuation-dissipation relations," Physica A **391**, 3585 (2012).
[38] F. Lechenault, G. Pallares, M. George, C. Rountree, E. Bouchaud, and M. Ciccotti, "Effects of Finite Probe Size on Self-Affine Roughness Measurements," Phys. Rev. Lett. **104**, 025502 (2010).
[39] S. G. Alves, C. I. L. de Araujo, and S. C. Ferreira, "Hallmarks of the Kardar-Parisi-Zhang universality class elicited by scanning probe microscopy," New J. Phys. **18**, 093018 (2016).